

RSC Advances



This is an *Accepted Manuscript*, which has been through the Royal Society of Chemistry peer review process and has been accepted for publication.

Accepted Manuscripts are published online shortly after acceptance, before technical editing, formatting and proof reading. Using this free service, authors can make their results available to the community, in citable form, before we publish the edited article. This *Accepted Manuscript* will be replaced by the edited, formatted and paginated article as soon as this is available.

You can find more information about *Accepted Manuscripts* in the [Information for Authors](#).

Please note that technical editing may introduce minor changes to the text and/or graphics, which may alter content. The journal's standard [Terms & Conditions](#) and the [Ethical guidelines](#) still apply. In no event shall the Royal Society of Chemistry be held responsible for any errors or omissions in this *Accepted Manuscript* or any consequences arising from the use of any information it contains.

Cadmium(II) complexes containing *N,N'*-dimethylvioluric acid as ligand or counteranion: Synthesis, characterization, crystal structures and DFT study

Cite this: DOI: 10.1039/x0xx00000x

Received 00th January 2012,
Accepted 00th January 2012

DOI: 10.1039/x0xx00000x

www.rsc.org/

Rupak Banik,^{†a} Subhadip Roy,^{†a} Antonio Bauza,^b Antonio Frontera^{*b} and Subrata Das^{*a,c}

N,N'-dimethylvioluric acid mono hydrate (HDMV) (**1**·H₂O) and two cadmium(II) complexes with N-donor ligands of formula [Cd(DMV)₂(Benzim)₂]·2H₂O (**2**) (Benzim= benzimidazole) and [Cd(H₂O)₄(py)₂](DMV)₂ (**3**) (py= pyridine) have been synthesized. Free *N,N'*-dimethyl violuric acid mono hydrate (HDMV) and the complexes have been fully characterized by elemental analysis, IR, ¹H and ¹³C NMR spectral methods, fluorescence spectroscopy, TGA and structural X-ray crystallography. HDMV (**1**·H₂O) which remains in keto-oxime form in solid state undergoes to nitroso-enolato form in the complexes [(**2**) and (**3**)]. A typical R₂(6) motif with a bifurcating hydrogen bond is observed in all the three structures. Dimethylviolurate anion acts as a bidentate ligand in (**2**), whereas in (**3**) it is present as a counter-ion, outside the coordination sphere. In addition, DFT-D₃ calculations have been performed to study interesting noncovalent interactions observed in the solid states of (**1**) and (**2**) with special interest to the lone pair(lp)–π interactions and their interplay with π–π interactions.

Introduction

Even at low levels cadmium is an extremely toxic heavy metal that can cause hepato, renal and neurotoxicity.¹⁻³ But normal human adult body usually contains some milligrams of it,⁴ mainly in metallothioneins, where it is bound to cysteinyl sulfur atoms.⁵ In a newly discovered carbonic anhydrase the cadmium(II) ion is also found to serve as the catalytic centre.⁶ In past few decades, cadmium(II) coordination complexes have attracted considerable attention due to their widely reported bioactivities, such as DNA binding ability,⁷ antibacterial activities⁸ and antitumor properties.^{9,10} Examples of applied cadmium coordination chemistry also include wastewater treatment and dealing with organic separation problems.^{11,12} Researchers around the world continue to employ ¹¹³Cd NMR spectroscopy as a “spin spy” in the study of various Zn^{II}-containing proteins.¹³ On the other hand, due to its d¹⁰ configuration with no CFSE, cadmium(II) can display a flexible geometry with possible coordination numbers ranging from four to eight, corresponding to different geometries. The

geometries and coordination numbers of cadmium(II) are generally governed by the steric needs of the ligands.¹⁴⁻¹⁷ This fact also makes Cd^{II} a key “player” in the fields of Crystal Engineering and Metallo-supramolecular Chemistry.^{18,19}

In addition, violuric acid is a derivative of barbituric acid containing an isonitroso group as a substituent. Many transition and s-block metal complexes of violuric acid are reported in literature.²⁰⁻²⁵ The nitrogen atom of the isonitroso group and the exocyclic oxygen atoms attached with the ring impart violuric acid with good ligating property. In coordination compounds, violurato derivatives show π-acceptor properties acting as strong-field ligands.²⁶ Violuric acid and its derivatives find applications in analytical purposes for the identification and determination of metal cations.²⁷ These are also used as antibacterial and antifungal agents²⁸ and display applications as redox mediators in enzymatic treatment of organic pollutants of wastewater.²⁹ Against cell lines human neuroblastoma (NB69), human glioma (U373-MG) and three other human tumour cell lines HL-60, BV-173 and SKW-3, violuric acid derivatives and complexes have been shown to exert moderate antiproliferative activity.³⁰⁻³¹

N,N'-dimethylvioluric acid, besides being a polydentate ligand, also possesses hydrogen bond donor and acceptor sites. Moreover, in its structure the presence of a pyrimidine ring favours π -stacking interactions. Hence, it can be employed as a building block for the construction of supramolecular assemblies. Although crystal structures of several metal complexes of *N,N'*-dimethylvioluric acid have been reported,^{26,32-36} the structure of the free ligand (or any other *N*-alkyl violuric acid derivative) has not been determined earlier. The use of nitrogenous ligands as building blocks in supramolecular chemistry is very well-known; in this work we have used benzimidazole and pyridine. Herein, we report the syntheses, crystal structures, spectroscopic and DFT studies of *N,N'*-dimethylvioluric acid mono hydrate and two new cadmium(II) complexes viz. $[\text{Cd}(\text{DMV})_2(\text{Benzim})_2] \cdot 2\text{H}_2\text{O}$ and $[\text{Cd}(\text{H}_2\text{O})_4(\text{py})_2](\text{DMV})_2$.

Experimental

Materials and methods

Reagents for synthesis were purchased as reagent grade and were used without further purification. Elemental analyses were carried out in a Perkin Elmer CHN analyzer (2400 series II). Infrared (IR) spectra were recorded as KBr disks using a Perkin-Elmer Spectrum 100 FT-IR spectrometer. ¹H-NMR and ¹³C-NMR spectra were recorded on a JNM ECS 400 MHz NMR spectrophotometer (JEOL) using tetramethylsilane (TMS) as the internal standard. Thermogravimetric analyses (TGA) of the samples were conducted using Shimadzu TG 50 thermogravimetric analyser with a heating rate of 10°C min⁻¹ under nitrogen atmosphere. Fluorescence emission spectra were recorded in H₂O using Shimadzu Spectrofluorophotometer RF-5000. The fluorescence quantum yield of the compounds was determined using 2-aminopyridine as a reference.³⁷ The compound and the reference were excited at the same wavelength maintaining nearly equal absorbance and the emission spectra were recorded. The area of the emission spectrum was integrated and the quantum yield was calculated according to the following equation:

$$\frac{\phi_S}{\phi_R} = \left[\frac{A_S}{A_R} \right] \times \left[\frac{(\text{Abs})_R}{(\text{Abs})_S} \right] \times \left[\frac{\eta_S^2}{\eta_R^2} \right]$$

Here, ϕ_S and ϕ_R are the fluorescence quantum yield of the sample and reference, respectively. A_S and A_R are the area under the fluorescence spectra of the sample and the reference respectively, $(\text{Abs})_S$ and $(\text{Abs})_R$ are the respective optical densities of the sample and the reference solution at the wavelength of excitation, and η_S and η_R are the values of refractive index for the respective solvent used for the sample and reference.

Synthetic part

Synthesis of HDMV (1·H₂O). HDMV was prepared according to a procedure described in literature.³² Yield: 89%. Elemental

anal. Calcd (%) for C₆H₉N₃O₅: C, 35.47; H, 4.46; N, 20.68. Found: C, 35.39; H, 4.53; N, 20.72. IR (cm⁻¹): 937v(N–O), 1675v(C=O), 1725 v(C=O), 3503v(H₂O); ¹H-NMR (DMSO-d₆): δ (ppm) 3.11 (s, N–CH₃), 3.17 (s, N–CH₃); ¹H-NMR (CDCl₃): δ (ppm) 3.11 (s, N–CH₃), 3.18 (s, N–CH₃); 14.50 (s, C5–N–OH); ¹³C-NMR (DMSO-d₆): δ (ppm) 27.61 (C3), 28.28 (C5), 135.69 (C1), 150.69 (C4), 153.59 (C2), 158.26 (C6).

Synthesis of $[\text{Cd}(\text{DMV})_2(\text{Benzim})_2] \cdot 2\text{H}_2\text{O}$ (2). An aqueous solution (20 mL) containing 0.5 mmol of cadmium(II) nitrate was added, slowly with stirring to 1 mmol of *N,N'*-dimethylvioluric acid and 1 mmol of benzimidazole, both dissolved in 15 mL methanol. The reaction mixture was stirred at room temperature for ~3 h, filtered to remove any undissolved residue, and kept at room temperature for several days when pink crystals were formed. Yield: 55% based on Cd. Elemental anal. Calcd (%) for C₂₆H₂₄CdN₁₀O₈: C, 41.47; H, 3.75; N, 18.6; Found: C, 43.35; H, 3.42; N, 19.44; IR (cm⁻¹): 1463v(N=O), 1606v(C=O), 1662v(C=O), 1717v(C=O), 3165v(N–H), 3402v(H₂O); ¹H-NMR (DMSO-d₆): δ (ppm) 3.10 (s, N–CH₃), 3.21 (s, N–CH₃), 7.20–7.21 (m, ArH), 7.60–7.61 (m, ArH), 8.27 (s, ArH); ¹³C-NMR (DMSO-d₆): δ (ppm) 26.32(C6), 28.54(C5), 108.30(C10), 120.80(C8), 122.03(C7), 137.60(C1), 142.30(C13), 167.54(C4), 170.40(C3), 176.46(C2).

Synthesis of $[\text{Cd}(\text{H}_2\text{O})_4(\text{py})_2](\text{DMV})_2$ (3). To a methanolic solution (25mL) of *N,N'*-dimethylvioluric acid (1mmol) was added 10 mL aqueous solution of cadmium(II) nitrate (0.5 mmol) and 0.5 mL of pyridine. The resulting solution was stirred at room temperature for ~6 h, filtered and left to evaporate at room temperature. By evaporation for several days, pink crystals were formed. Yield: 74% based on Cd. Elemental anal. Calcd (%) for C₂₂H₃₀CdN₈O₁₂: C, 37.16; H, 4.25; N, 15.76. Found: C, 37.26; H, 4.28; N, 15.66. IR (cm⁻¹): 629 ρ_w (H₂O), 753 ρ_r (H₂O), 1010-825v(C–H out-of-plane), 1223–1085v(C–H in-plane), 1261v(C–O), 1471 v(N=O), 1654v(C=O), 1726v(C=O), 3510v(H₂O)); ¹H-NMR (DMSO-d₆): δ (ppm) 3.07 (s, N–CH₃), 3.29 (s, N–CH₃), 7.43–7.44 (m, ArH), 7.82–7.84 (m, ArH), 8.54–8.55 (d, ArH); ¹³C-NMR (DMSO-d₆): δ (ppm) 26.4(C9), 28.3(C11), 124.36(C2), 135(C3), 137.5(C4), 149.1(C1), 159.95(C8), 163.82(C10), 168.02(C6).

Crystal data collection and refinement

Intensity data of **1·H₂O**, **2** and **3** were collected on a Bruker SMART APEX CCD area detector system [$\lambda(\text{Mo-K}\alpha)=0.71073\text{\AA}$] at 296 K using graphite monochromator with ω scan. Crystal cell refinement and data reduction were carried out using Bruker SAINT.³⁸ Absorption effects in the compounds were corrected using SADABS.³⁹ Using Olex2,⁴⁰ structures were solved with the olex2.solve structure solution program, using the Charge Flipping solution method. The models were refined with the ShelXL-2013⁴¹ refinement package using Least Squares minimisation. All non-hydrogen atoms were refined anisotropically. Hydrogen positions were calculated geometrically and refined using the riding model. In

the structure of **1**·H₂O, the isonitroso group is disordered over two positions with refined occupancies of approximately 58:42 for the major and minor disorder components. In **1**·H₂O, the U_{anis} values of atoms N1B and N1A have been constrained to be identical (EADP) and restraints have been used to keep the distances C1-N1B/N1A as well as those between N1A-O1A/N1B-O1B the same (SADI). For complex **2**, the electron density present in the voids is highly disordered and it was not possible to obtain an atomic model. The solvent masking procedure available from PLATON/SQUEEZE⁴² was used to calculate the size of the voids and to estimate the residual electron density and revealed the presence of two water molecules per complex. The crystallography data of compound **1**·H₂O, **2** and **3** are summarized in Table 1.

Theoretical methods

The energies of all complexes included in this study were computed at the BP86-D3/def2-TZVP level of theory. The geometries have been fully optimized unless otherwise noted. For instance to evaluate the noncovalent interactions observed in the solid state, we have used the crystallographic coordinates. The calculations have been performed by using the program TURBOMOLE version 6.5.⁴³ For the calculations we have used the BP86 functional with the latest available correction for dispersion (D3).⁴⁴ For **1**·H₂O, only the major component of the disordered isonitroso group was considered for DFT calculations.

Results and discussion

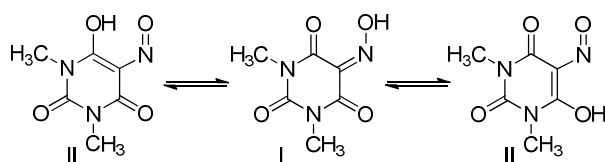
Synthesis

Generally, in a strong acid medium hydrolysis of 6-amino-1,3-dimethyl-5-nitrosouracil (HDANU) occurs to produce HDMV and it is a common process reported in literature.³² It is also found that substitution on the amino group facilitates this process.³⁶ An alternative method for preparation of HDMV is the treatment of 1,3-dimethylbarbituric acid with nitrous acid.⁴⁵ In a literature report a three component reaction involving copper(II) perchlorate or copper(II) chloride, HDANU and 2,2'-bipyridine in EtOH/water medium yielded mixed ligand complexes [Cu(DANU)(bipy)(H₂O)]ClO₄·H₂O and [Cu(DMV)(bipy)Cl]·0.5H₂O.⁴⁶ Though formation of the former complex is unexceptional but in case of latter existence of the in-situ HDMV (*N,N'*-dimethylvioluric acid) ligand proceeded from the HDANU hydrolysis. In the present study acid hydrolysis of 6-amino-1,3-dimethyl-5-nitroso uracil with HCl was carried out to yield HDMV which was fully characterized and then reacted with cadmium(II) nitrate tetrahydrate and benzimidazole/pyridine in aqueous methanolic solution at room temperature to produce two novel metal complexes (**2** and **3**). The complexes have been characterized by routine physicochemical techniques as well as by X-ray single-crystal structure analysis. It is important to mention here that the ligand HDMV contains one ionizable proton that can be involved in a ketoneoxime ⇌ nitrosoenol tautomeric equilibrium (Scheme 1),^{35,36} but single

Table 1 Selected crystallographic data for compounds **1**·H₂O, **2** and **3**

	C ₆ H ₉ N ₃ O ₅ (1 ·H ₂ O)	C ₂₆ H ₂₈ CdN ₁₀ O ₁₀ (2)	C ₂₂ H ₃₀ CdN ₈ O ₁₂ (3)
Empirical formula	C ₆ H ₉ N ₃ O ₅ (1 ·H ₂ O)	C ₂₆ H ₂₈ CdN ₁₀ O ₁₀ (2)	C ₂₂ H ₃₀ CdN ₈ O ₁₂ (3)
Formula weight	203.16	752.98	710.94
Temperature/K	296(2)	296(2)	296(2)
Crystal system	monoclinic	trigonal	triclinic
Space group	P2 ₁ /n	R-3c	P-1
a/Å	8.3766(8)	27.5068(12)	8.4597(5)
b/Å	6.2427(6)	27.5068(12)	9.1787(5)
c/Å	17.4768(17)	24.343(2)	10.2999(6)
α/°	90	90	88.351(2)
β/°	102.314(6)	90	85.190(2)
γ/°	90	120	62.638(2)
Volume/Å ³	892.88(15)	15950.9(19)	707.75(7)
Z	4	18	1
ρ _{calc} /cm ³	1.511	1.411	1.668
μ/mm ⁻¹	0.133	0.679	0.848
F(000)	424.0	6876.0	362.0
Crystal size/mm ³	0.47 × 0.12 × 0.08	0.54 × 0.124 × 0.121	0.3 × 0.1 × 0.1
Radiation	MoKα (λ = 0.71073)	MoKα (λ = 0.71073)	MoKα (λ = 0.71073)
2θ range for data collection/°	4.772 to 51.99	4.784 to 60.12	4.998 to 51.996
	-10 ≤ h ≤ 10	-37 ≤ h ≤ 38	-10 ≤ h ≤ 10
Index ranges	-7 ≤ k ≤ 7	-38 ≤ k ≤ 38	-11 ≤ k ≤ 11
	-21 ≤ l ≤ 21	-33 ≤ l ≤ 34	-12 ≤ l ≤ 12
Reflections collected	7970	153107	12467
Independent reflections	1753 [R _{int} = 0.0238, R _{sigma} = 0.0180]	5189 [R _{int} = 0.0547, R _{sigma} = 0.0224]	2766 [R _{int} = 0.0250, R _{sigma} = 0.0166]
Data/restraints/parameters	1753/2/144	5189/0/204	2766/12/215
Goodness-of-fit on F ²	1.046	1.113	1.218
Final R indexes [I ≥ 2σ (I)]	R ₁ = 0.0495, wR ₂ = 0.1397	R ₁ = 0.0368, wR ₂ = 0.0856	R ₁ = 0.0231, wR ₂ = 0.0644
Final R indexes [all data]	R ₁ = 0.0563, wR ₂ = 0.1490	R ₁ = 0.0672, wR ₂ = 0.1045	R ₁ = 0.0233, wR ₂ = 0.0646
Largest diff. peak/hole /eÅ ⁻³	0.33/-0.21	0.53/-0.33	0.43/-0.48

crystal diffraction confirmed the presence of the tautomeric ketone-oxime form for free acid (HDMV) in solid state.



Scheme 1 Tautomeric equilibrium in HDMV

Crystal structure of $1 \cdot H_2O$

The structure of free ligand *N,N'*-dimethylvioluric acid monohydrate [$1 \cdot H_2O$], has bond distances and angles that are largely unexceptional. The only exception is the deviation of the exocyclic angles at atom C1 from the ideal trigonal value of 120° . The molecular structure is shown in Fig. 1. In the structure the isonitroso group is disordered over two positions; the occupancies are competitively refined to 58:42 ratio. This disorder is not unprecedented in literature and a common occurrence for violuric acid and other related compounds.^{36,47} In violuric acid, an $R^2_2(8)$ hydrogen bonding motif between N-H and C=O groups typically leads to sheet-like structures.⁴⁷⁻⁵⁰ Since this bonding motif is not possible in $1 \cdot H_2O$, we were interested in investigating how the presence of *N*-substituents affects the crystal packing of $1 \cdot H_2O$.

Considering only the major part of the disordered isonitroso group, co-crystallized water forms a $R^2_1(6)$ motif with **1**, with a bifurcating hydrogen bond of H5D with two oxygen atoms O1A and O4, (Fig. 2, Table 2). The same motif, containing a bifurcating hydrogen donor, is found in the water and methanol adducts of violuric acid.⁴⁷⁻⁵⁰

Table 2 Geometrical parameters of hydrogen-bonding interactions in $1 \cdot H_2O$

D	H	A	d(D-H)/Å	d(H-A)/Å	d(D-A)/Å	D-H-A $^\circ$
O1A	H1A	O5	0.82	1.72	2.534(3)	171.1
O1B	H1B	O5	0.82	1.80	2.617(5)	176.7
O5	H5D	O1A1	0.85	2.19	2.807(3)	129.1
O5	H5D	O41	0.85	2.08	2.809(2)	142.9
O5	H5E	O22	0.85	1.93	2.752(2)	163.7

$$^1 1 - x, 2 - y, 1 - z; ^2 2 - x, 2 - y, 1 - z$$

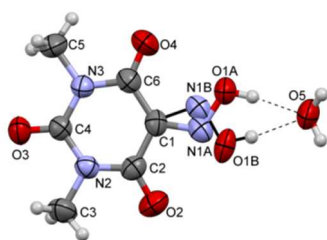


Fig. 1 Crystal structure of $1 \cdot H_2O$. Thermal ellipsoids are drawn at 50% probability.

In the structure inversion symmetry leads to a $R^4_4(8)$ motif (O1A, O5 and symmetry equivalents) and the formation of a hydrogen-bonded water-bridged dimer. Again, the structure shows high similarity to the methanol adduct of violuric acid, in which the same $R^4_4(8)$ motif was formed between two molecules of violuric acid and two molecules of methanol.⁴⁷ However, while involvement of NH group in further hydrogen bonding causes the formation of a two-dimensional sheet structures for violuric acid, this is not possible for **1**. Instead, only the co-crystallized water molecule is involved in further hydrogen bonding, resulting in one-dimensional chains parallel to the *a*-axis, connected by a $R^4_4(16)$ motif involving O1A, O2 and O5 (Fig. 2). Since the *N*-methyl groups prevent the formation of a two-dimensional layered structure, chains of dimeric **1** form tilted stacks along the *b*-axis (Fig. S1 in the ESI †). Perpendicular (C4=)O4–C4'(=O3') interactions are observed between stacks with a distance of 2.9 Å. Similar interactions with a (C=)O–C'(=O') distances of 3.0–3.2 Å were observed in *N,N'*-dimethylbarbituric acid, which likewise was unable to form a 2D-sheet structure due to the *N*-substitution.⁵¹ For the lower (42%) occupancy of the disordered isonitroso group, the $R^2_1(6)$ motif with the bifurcating O5-H5D hydrogen bond and $R^4_4(8)$ motif are replaced by a straightforward $R^4_4(16)$ motif (Fig. 3). Since the isonitroso group does not participate in other hydrogen bonding than the formation of the water-bridged dimer, its disorder does not have any impact on the crystal packing.

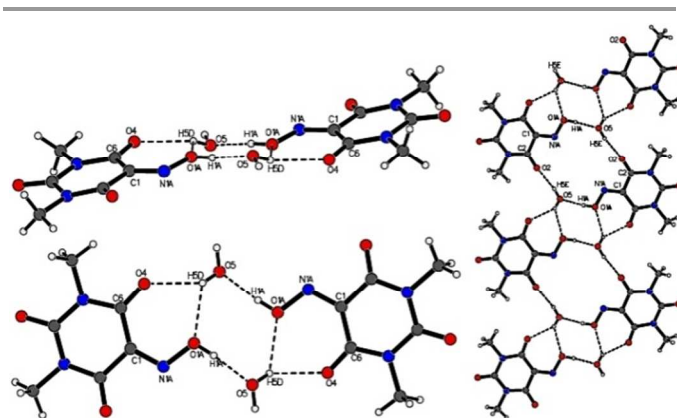


Fig. 2 Left: Hydrogen-bonded dimer of **1** bridged by co-crystallized water. Right: One-dimensional chains of the hydrogen-bonded dimers of **1**. The minor disorder component has been ignored.

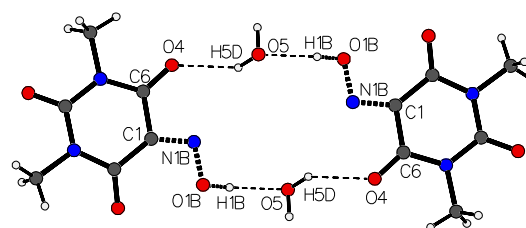


Fig. 3 The hydrogen bonded dimer ($1 \cdot H_2O$)₂ using the minor component of the disordered isonitroso group.

Crystal structures of **2** and **3**

Given the strong implication of the isonitroso group in hydrogen bonding in the free *N,N'*-dimethylvioluric acid, we were interested to explore the respective hydrogen-bonding network of inner- and outer-sphere ion pairs of the dimethylviolurate anion. Thus we determined structures of cadmium complexes **2** and **3**, the former containing a metal-coordinated dimethylviolurate anion, the latter having a coordinatively saturated metal center and a non-coordinated dimethylviolurate anion. To the best of our knowledge, complex **2** is the first cadmium violurate coordination complex structurally characterised.

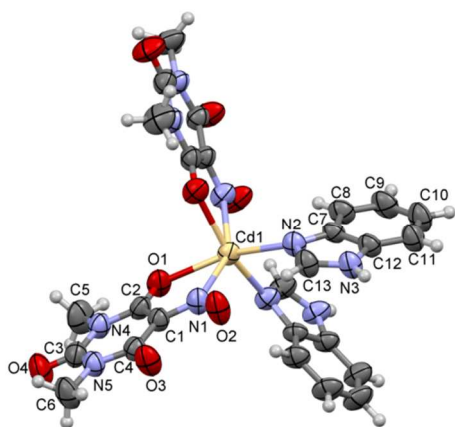


Fig. 4 The crystallographically derived structure of **2** (thermal ellipsoids are drawn with 50% probability)

Complex **2** crystallizes as a distorted octahedron with crystallographic C_2 -symmetry. Molecular view of the complex is shown in Fig. 4. As typically observed, metal coordination is achieved via coordination of the *N*-atom of the NO-group, to form a five-membered metallacycle. The reduced bite angle of the dimethylviolurate ligand [O–Cd–N=68.32(7)°] results in distortion from ideal octahedral geometry with coordination angles ranging from 69° to 107°. The two ancillary benzimidazole ligands are in *cis*-position, in contrast to other bis(violurate) complexes containing monodentate ancillary ligands, *trans*-(violurate)₂Cu(OH₂)₂^{32,36,52,53} and *trans*-(violurate)₂Co(OH₂)₂.⁵⁴ The configuration of the latter two complexes is, however, more likely a consequence of their d^7 - and d^9 -metal centers, than caused by a difference between benzimidazole and water as a ligand. The Cd1–N2 bond distance [2.286(2) Å] falls within the range of values typically observed in six-coordinate Cd benzimidazole complexes [2.22–2.37 Å, 19 structures].⁵⁵ The dimethylviolurate ligand displays a N1–O2 bond which is significantly shorter [1.265(3) Å] than the corresponding N–OH bond distance in dimethylvioluric acid monohydrate (**1**·H₂O) [1.356(4) Å], indicating strong double bond character of the N–O bond. The C1–N1 distance of 1.337(3) Å is, however, notably shorter than the distance of 1.35–1.40 Å expected for a κ_N -coordinated aromatic C–nitroso complex.⁵⁶ This, together with slightly shorter C1–C2 and

slightly longer C2–O1 distances in **2** compared to the free acid, indicate some degree of delocalisation of the negative charge to the metal coordinated oxygen atom. O2 and O3 of the dimethylviolurate ligand, together with H3 of benzimidazole from a neighbouring molecule related by a C_2 -axis, form the hydrogen-bonded $R^2_1(6)$ motif already observed in the crystal structure of the free acid **1**·H₂O. Combined with the crystallographic C_2 -symmetry of the molecules, this leads to the formation of 1D-hydrogen-bridged chains (Fig. 5, Table 3) parallel to the *c*-axis, in which each complex is connected via four $R^2_1(6)$ motifs to its neighbours.

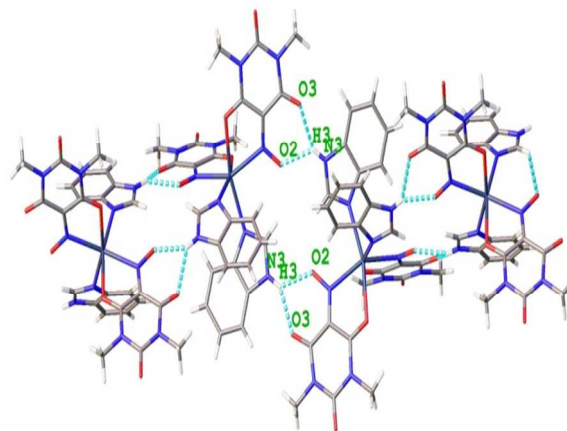


Fig. 5 Hydrogen-bridged one-dimensional chains parallel to the *c*-axis.

Further packing interactions between the 1D-chains involve intermolecular carbonyl– π interactions between O4 and dimethylviolurate and π -stacking interactions between dimethylviolurate and benzimidazole. The latter is most likely responsible for the slightly bent coordination of the benzimidazole ligand.

The total solvent-accessible volume of the unit cell is 3837.3 Å³, which is 24.05 % of the unit cell volume. Fig. 6 was obtained during the solvent masking procedure available from SQUEZE/PLATON.

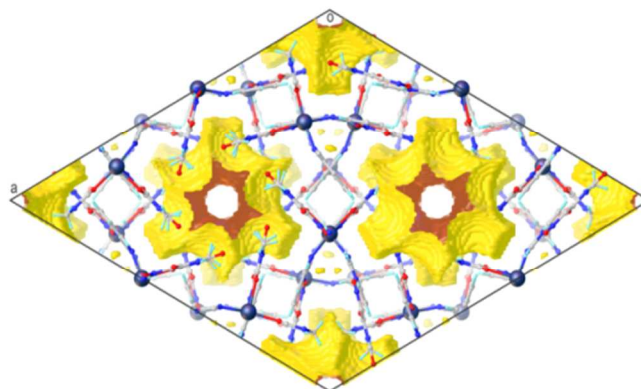


Fig. 6 A view of the unit cell along the *c* reveals two of the three symmetry-equivalent channels that run through this structure. The third channel is composed of partial channels along the cell edges.

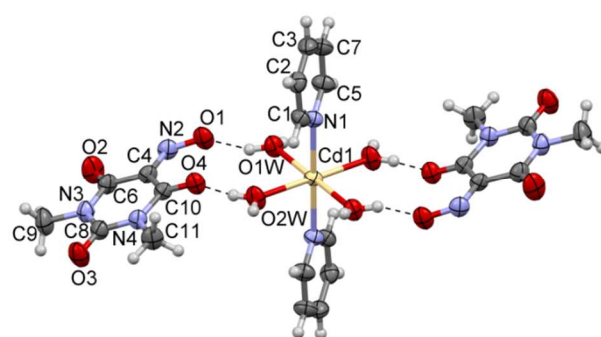
Table 3. Geometrical parameters of hydrogen-bonding interactions in **2**

D	H	A	d(D-H)/Å	d(H-A)/Å	d(D-A)/Å	D-H-A/°
N3	H3	O2 ¹	0.858(2)	2.142(2)	2.839(3)	138.14(15)
N3	H3	O3 ¹	0.858(2)	2.116(2)	2.826(3)	139.84(16)
C13	H13	O2 ²	0.930(2)	2.2891(19)	3.030(3)	136.29(18)

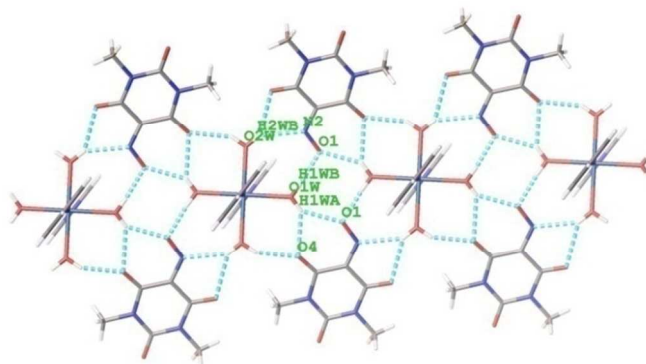
$$^1/2/3+y-x,4/3-x,1/3+z; ^2/2/3-y+x,4/3-y,5/6-z$$

In complex **3** dimethylviolurate forms an outer-sphere ion pair with a coordinatively saturated metal cation, here $[(C_5H_5N)_2Cd(OH_2)_4]^{2+}$, which crystallizes with crystallographic inversion symmetry. Molecular view of the complex is shown in Fig. 7. Bond distances and angle of the octahedral cadmium cation fall well in the normal range observed in octahedral cadmium complexes [Cd-OH₂: 2.32(4) Å, 1225 structures; Cd-py: 2.37(4) Å, 55 structures].⁵¹ As in the metal-coordinated dimethylviolurate in **2**, bond distances in the non-coordinated dimethylviolurate anion indicate some degree of delocalisation of the negative charge to oxygen O4, which is involved in hydrogen bonding interactions. Hydrogen bonding between the dimethylviolurate anion and the cadmium-bound water molecules leads, again, to the formation of one-dimensional chains, parallel to the *a*-axis (Fig. 8, Table 4). One water molecule forms a bifurcating hydrogen bridge involving H1WA and oxygen atoms O1 and O4 of the dimethylviolurate anion, giving rise to same $R^2_1(6)$ motif observed in the crystal structure of the free acid (**1**·H₂O) and in **2**. A second water molecule of the same cation forms a $R^1_2(6)$ motif, with H2WA, H1WA and O4. Bridging interaction of the oxime group (N2 and O1) with a neighbouring cation forms a $R^2_2(7)$ motif involving H2WB and H1WB. Finally, the presence of a second bridging dimethylviolurate anion related by inversion symmetry, forms a central $R^2_4(8)$ motif involving hydrogens H1WA and H1WB of two cations and O1 of two anions. Packing of the chains along the *b*-axis (Fig. S2 in the ESI†) involves π -stacking between the pyridine rings and π -stacking between dimethylviolurate anions (strongly shifted).

In summary, strong hydrogen bonding is observed in all three structures. In all cases, the NO group of dimethylvioluric acid/dimethylviolurate is involved in formation of a typical $R^2_1(6)$ motif with a bifurcating hydrogen bond to the NO group and a neighbouring CO group. In fact, the same motif can be found in most other dimethylviolurate structures in the presence of slightly acidic hydrogens, such as for example (DMV)₂Cu(OH₂)₂,³² [(DMV)₃Fe][Fe(OH₂)₆]·H₂O,³³ [(DMV)₃Ru][H₃O]·H₂O,³⁴ or [(DMV)Re(CO)₃(OH₂)₂].³⁵

**Fig. 7** Molecular view of the complex **3** (thermal ellipsoids are drawn with 50% probability).**Table 4** Geometrical parameters of hydrogen-bonding interactions in **3**

D	H	A	d(D-H)/Å	d(H-A)/Å	d(D-A)/Å	D-H-A/°
O1W	H1WA	O1	0.822(8)	2.086(17)	2.784(2)	143(2)
O1W	H1WA	O4	0.822(8)	2.280(16)	2.9602(19)	140(2)
O2W	H2WA	O4	0.822(8)	2.094(15)	2.843(2)	151(3)
O2W	H2WB	O21	0.822(8)	2.37(2)	3.048(2)	141(3)
O2W	H2WB	N21	0.822(8)	2.186(16)	2.910(2)	147(3)
O1W	H1WB	O12	0.822(8)	1.880(8)	2.699(2)	174(2)

**Fig. 8** Hydrogen bonding network leading to one-dimensional chains of dimethylviolurate bridged cadmium cations.

Theoretical study

The theoretical study is focused to the analysis of the interesting noncovalent interactions observed in the solid state architecture of **1**·H₂O and **2** with special interest to the lone pair(lp)- π interactions (see Fig. 9A and B). Both compounds exhibit very short lp- π contacts (< 2.90 Å) that are expected to be strong due to the electronic nature (π -acidity) of the six membered ring of dimethylvioluric acid. We have also studied the hydrogen bonded tetramer involving two *N,N'*-dimethylvioluric acid and two water molecules (Fig. 9C). Moreover, we have analyzed the formation of the self-assembled hexameric structure observed in compound **2** where six simultaneous lp- π / π -assemblies are formed (Fig. 9A).

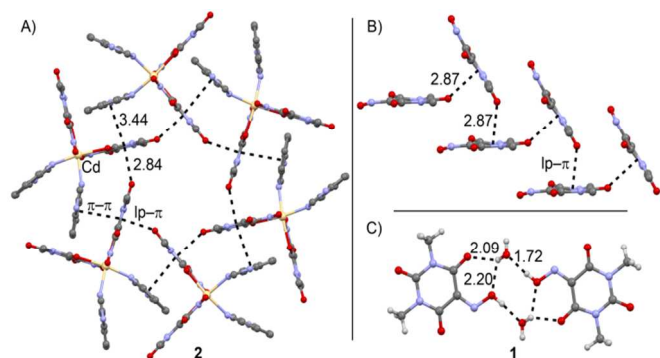


Fig. 9 X-ray structures of compounds **1**·H₂O (right) and **2** (left).

First we have focused our attention to the position of the hydrogen atom of the hydroxyl group that, surprisingly, it is not forming an intramolecular O–H···O=C hydrogen bonding. We have optimized both possibilities at the BP86-D3/def2-TZVP level of theory and, as expected, the conformer that present the intramolecular H-bond is 7.9 kcal/mol more stable (Fig. 10) than the other one. As aforementioned the hydroxyl group participates as an H-donor/acceptor group in the formation of a tetrameric assembly in the solid state where six H-bonds are formed. The interaction energy for this assembly (using the X-ray coordinates) is $\Delta E_{\text{int}} = -21.0$ kcal/mol that largely compensates 15.8 kcal/mol required to stabilize two violuric acid moieties in a conformation where the intramolecular H-bond is not formed. We have also optimized this tetrameric assembly starting from the X-ray coordinates. Interestingly, it is also stable in the gas phase, indicating that it is a strong binding motif in the solid state of **1**·H₂O. The interaction energy is much larger (in absolute value) in the optimized tetramer than in the X-ray structure because some H-bonds are shorter. This is due to the absence in the gas phase optimization of the additional interactions with the neighboring molecules that are present in the solid state.

We are also interested in studying the influence of the conformation adopted by the violuric acid on the π -binding ability of the ring. Therefore we have computed the molecular electrostatic potential (MEP) surface of compound **1**·H₂O, exploring several conformations and complexes (see Fig. 11). The energetic value at the π -hole (region of positive electrostatic potential over the ring) is more positive when the intramolecular H-bond is formed (5 kcal/mol). Interestingly, when a water molecule is included in the calculation of the MEP in the same position that is found in the crystal structure, the energetic value at the π -hole is identical to the conformer with the intramolecular H-bond. Therefore the ability of the ring to establish lp- π interactions is enhanced by the presence of the water molecule.

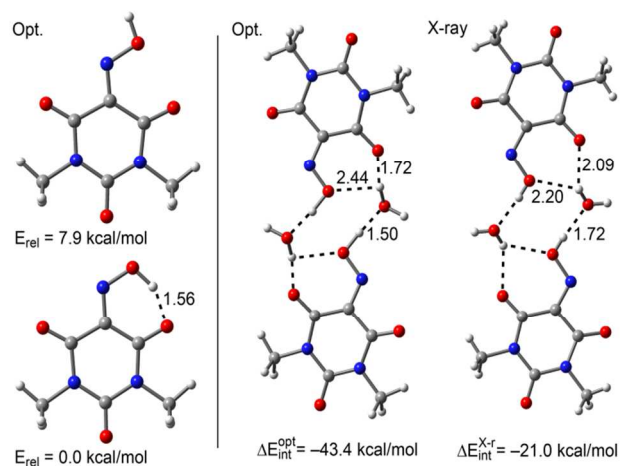


Fig. 10 Left: BP86-D3/def2-TZVP optimized geometries of two conformers of compound **1**. Relative energies are also indicated. Right: Interaction energies of the tetrameric assembly using both X-ray and optimized coordinates. Distances in Å

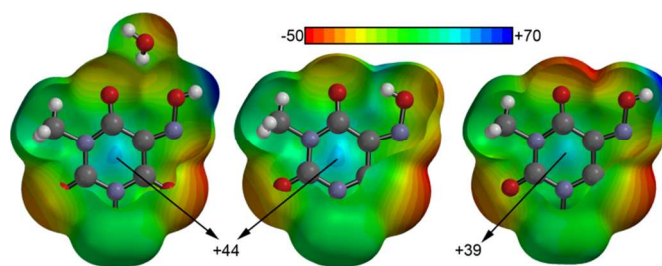


Fig. 11 Molecular Electrostatic Potential surfaces of compound (**1**·H₂O) in two conformations (right, middle) and interacting with a water molecule (left)

Finally, we have computed the interaction energy of the lp- π complex that is crucial to explain the solidstate architecture of compound **1**·H₂O (Fig. 9, top-right). We have evaluated the interaction using two theoretical dimers (Fig. 12) in order to evaluate the two contributions to the total binding energy. That is, in the lp- π complex observed in the solid state there are two secondary interactions (C–H···O=C) that have been represented using green dashed lines in (Fig. 12). In order to evaluate the lp- π without the contribution of these interactions we have used a model where the methyl groups have been replaced by hydrogen atoms in the lp donor molecule. The interaction energy of this model $\Delta E_2 = -5.0$ kcal/mol that corresponds to the lp- π interaction and the difference $\Delta E_1 - \Delta E_2 = -3.0$ kcal/mol corresponds to the contribution of both C–H···O=C secondary interactions. We have also computed these binding energies using the MP2 level of theory and the same basis set in order to assess the quality of the energies calculated with the dispersion corrected functional. The values are shown in parenthesis in Fig. 12 and a good agreement is found. The contribution of both C–H···O=C secondary interactions at this level of theory is 2.1 kcal/mol that is slightly lower than the

value obtained at the DFT-D3 level. The lp- π interaction energy is identical at both levels of theory (-5.0 kcal/mol).

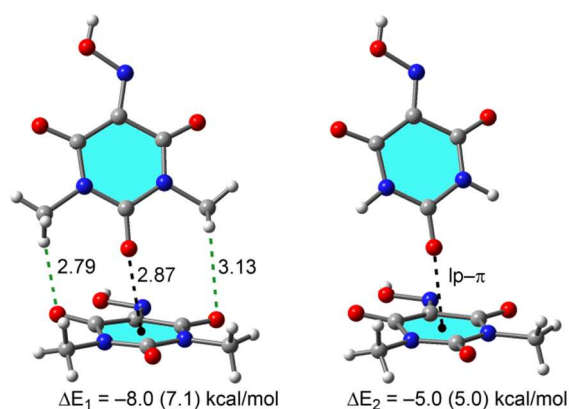


Fig. 12 Theoretical models used to evaluate the different contributions to the total interaction energy (MP2 values in parenthesis). Distances in Å.

In compound **2** we have focused our attention to evaluate the energetic contributions of the different noncovalent interactions that are involved in the formation of the fascinating hexameric assembly (Fig. 9A). Remarkably, the geometric features of lp- π interaction are almost equivalent in both compounds (**1**·**H₂O** and **2**). Taking into consideration that **2** is totally different (a transition metal coordination complex where *N,N'*-dimethylviourate and benzimidazole coexist as coligands), the existence of the same binding motif in the solid state clearly indicates that it is an important supramolecular synthon. The different X-ray fragments and theoretical models used to analyze the interactions in compound **2** are shown in Fig. 13. In the left part (Fig. 13A) we show the elementary fragment that generates the hexameric self-assembly. It is stabilized by a

combination of lp- π , π - π and secondary (C-H...O=C) interactions that have been represented using green dashed lines. The interaction energy of this complex is large and negative, $\Delta E_3 = -21.4$ kcal/mol. The other two theoretical models used to evaluate the individual contribution of each interaction are also shown in Fig. 13 (B and C). In the model shown in Fig. 13 B we have replaced the methyl groups by hydrogen atoms in the lp donor moiety (one viourate ligand) and, as a result, the interaction is reduced to $\Delta E_4 = -16.8$ kcal/mol, indicating that the contribution of the H-bonds is $\Delta E_{\text{HB}} = \Delta E_3 - \Delta E_4 = -4.6$ kcal/mol, which is more favorable than the previously computed for compound **1**·**H₂O** (-3.0 kcal/mol, Fig. 12) likely due to the coordination of the oxygen atom to Cd metal center. In the last model (Fig. 13C), we have replaced the benzimidazole ligand by an HCN to eliminate the contribution of the π - π interaction. As a result the interaction energy is reduced to $\Delta E_5 = -13.5$ kcal/mol. By means of ΔE_3 , ΔE_4 and ΔE_5 interaction energies, the individual contributions of the lp- π and π - π interactions can be estimated. That is, $\Delta E_{\pi-\pi} = \Delta E_3 - \Delta E_5 = -7.9$ kcal/mol and $\Delta E_{\text{lp}-\pi} = \Delta E_3 - \Delta E_{\pi-\pi} - \Delta E_{\text{HB}} = -8.9$ kcal/mol. The stacking interaction is favored by the fact that the viourate ring is electron poor and the benzene ring of the benzimidazole is electron rich. Moreover the lp- π interaction is stronger than that computed for **1**·**H₂O** due to the influence of the coordination of the ligand to cadmium that enhances the π -acidity of the ring.

Finally, we have performed a search in the Cambridge Structural Database (CSD) in order to further analyze the π -binding ability of *N,N'*-dimethylviouric ring. It is well-known that the CSD is a convenient and reliable tool for analyzing geometrical parameters.⁵⁷ Interestingly, we have found only 14 X-ray structures where the *N,N'*-dimethylviourate ligand is coordinated to transition metals. In 12 out of 14 structures the ring participates in lp- π and anion- π interactions,⁵⁸ which is an

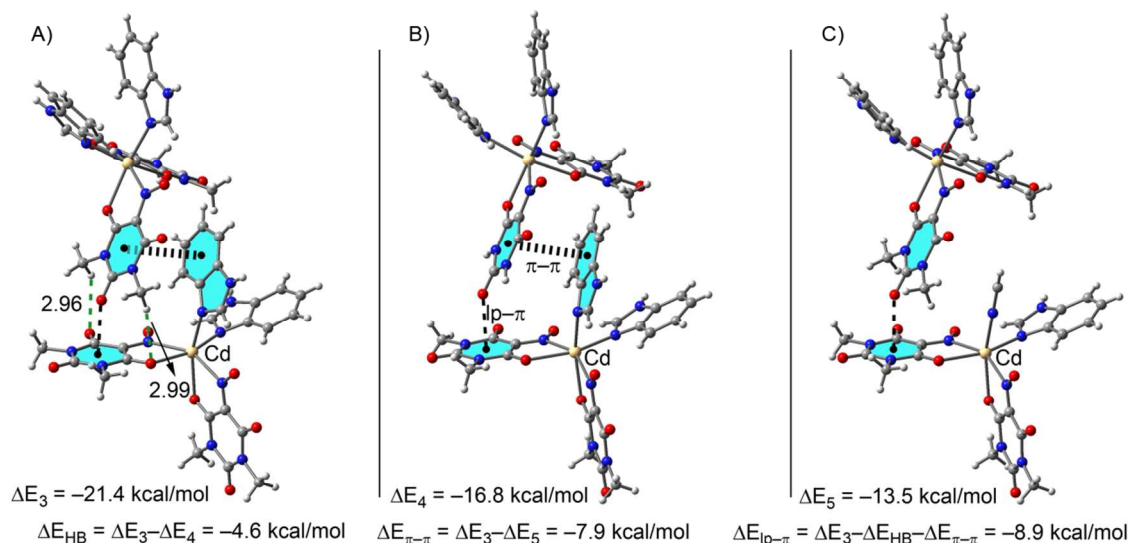


Fig. 13 Left: partial view of the crystal packing of compound **2** with indication of the different noncovalent interactions. The equations used to evaluate the energetic contributions are also shown. Distances in Å.

indication of the ability of this ring to interact with electron rich molecules. Some examples are shown in (Fig. S3, see ESI) illustrating the importance this interaction in the solid state. In one example (JIFBOP)³² the binding mode is very similar to the observed in compounds **1**·H₂O and **2** and generates a self-assembled dimer in the solid state (Fig. S3 left). In the other two selected examples the electron rich moiety is anionic (NIDHIR)⁵⁹ and YEVBK)⁶⁰ and the anion- π contacts are evident. The lp/anion- π interaction distances range 2.76–3.15 Å that are shorter than usual for this type of bonding.^{61,62} This result agrees well with the large binding energies obtained in the DFT energetic analysis (*vide supra*).

Spectral study

IR studies

A comparative study of the IR spectral data of the complexes with that of the free ligand gives supportive evidences towards better understanding of the coordinating behaviour of the ligand molecule. In the IR spectra of free ligand (**1**·H₂O), the appearance of a broad band at *ca.* 3503 cm⁻¹ indicates the presence of a hydrogen bonded water molecule, consistent with the single-crystal X-ray diffraction results. Among the 2-, 4- and 6-carbonyl groups (according to IUPAC nomenclature), the 4- and 6-carbonyl groups being substantially equivalent, the free ligand displays two bands at *ca.* 1725 and 1675 cm⁻¹ which may be assigned to coupled vibrational activity of carbonyl groups. In addition, the presence of a sharp band at *ca.* 937 cm⁻¹ is attributed to $\nu(\text{N-O})$ from the oxime group which further lends support to the single crystal X-ray studies that the free ligand (**1**·H₂O) remains in ketone-oxime form in solid state.

In case of complex **2**, the metal-ligand coordination through the oxygen atom of one carbonyl group is clearly indicated by the changes in the $\nu(\text{C=O})$ bands, which are all shifted to lower wavenumbers with respect to their position in the IR spectrum of the free ligand. Upon complexation, the 4- and 6-carbonyl groups remain no longer equivalent, and three bands at *ca.* 1717, 1662 and 1606 cm⁻¹ may be assigned to coupled vibrational activity of carbonyl groups. The appearance of a sharp band at *ca.* 1463 cm⁻¹ assignable to $\nu(\text{N=O})$ from the nitroso group is indicative of the fact that upon complexation, the ketone-oxime form of the free ligand no longer exists and completely becomes the nitroso-enolato one. In the spectrum, the band around 3165 cm⁻¹ is assignable to $\nu(\text{N-H})$ of benzimidazole ligands. A weak band⁶³ at *ca.* 3402 cm⁻¹ is tentatively assigned to O-H stretching of disordered solvate water molecules. Free benzimidazole ring system has strong absorption band in the range 1450–1650 cm⁻¹ for $\nu(\text{C=N})$ -stretching. But in the spectra of **2**, the band for $\nu(\text{C=N})$ could not be distinguished and could possibly be masked by the $\nu(\text{C=O})$ and $\nu(\text{N=O})$ vibrations from dimethylviolurate which also fall in the same region. The appearance of bands in the far IR region at 427–412 cm⁻¹ in the complex may be assignable to Cd-N frequency.

In the IR spectrum of **3**, the broad band around 3510 cm⁻¹ confirms the presence of water molecules. The IR spectrum

also shows bands corresponding to $\rho_r(\text{H}_2\text{O})$ (*ca.* 753 cm⁻¹) and $\rho_w(\text{H}_2\text{O})$ (*ca.* 629 cm⁻¹) which indicate the presence of coordinated water molecules. For coordinated pyridine molecules, the C-H out-of-plane bending falls in the FTIR values of *ca.* 1010–825 cm⁻¹. The C-H in-plane bending vibrations are assigned to the region *ca.* 1223–1085 cm⁻¹. We also observe two bands at about 1726 and 1654 cm⁻¹, which corresponds to the $\nu(\text{C=O})$ stretching vibration of the two carbonyl groups from the non-coordinated dimethylviolurate anion. The bands appearing at *ca.* 1471 and 1261 cm⁻¹ are mainly due to $\nu(\text{N=O})$ and $\nu(\text{C-O})$ vibrations which further confirm the single crystal X-ray studies that non-coordinated dimethylviolurate anion is present in nitroso-enolato form.

Thus, IR spectral data clearly lend support to the structures determined by X-ray diffraction method.

NMR studies

¹H-NMR and ¹³C-NMR spectra of HDMV (**1**·H₂O), **2** and **3** were recorded in DMSO-d₆. ¹H-NMR spectrum of HDMV was also recorded in CDCl₃. Due to high polarity of DMSO-d₆, ¹H NMR spectrum of free HDMV in DMSO-d₆ the peak related to exchangeable NOH proton is not observed which is otherwise observed at 14.5 ppm in CDCl₃. The ¹H NMR spectra of complex **2** and **3** show signals which are assignable to aromatic hydrogens of benzimidazole, pyridine and as well as DMV (dimethylviolurate). These signals undergo small shift with respect to the free ligands and provide evidence for coordination of ligands to metal. A comparison of the ¹³C NMR spectra of the complexes with those of the free ligands shows downfield shifts in the carbon signals upon complexation.

Thermal Studies

The stability of the compounds was studied by thermogravimetric analysis (TGA), see Figs S4–S6 (ESI). The degradation of free dimethylvioluric acid monohydrate molecule shows that dehydration of the acid starts at around 78°C and finishes at 133°C, yielding the anhydrous acid. The observed weight loss of 9.2% along this temperature range corresponds to one molecule of water. The theoretical value (8.9%) calculated from this elimination is in good agreement with the experimental value. Finally pyrolysis of violuric acid as volatile gases such as HCN, N₂, CO and CO₂ occurs at 165°C and finishes above 360 °C.

The TGA data indicates that complex **2** undergoes solvent-loss mass changes over 110–150°C (clathrated molecules). Further weight loss of 32.42% in temperature range 165–225°C occurs with release of two benzimidazole units which is close to the calculated value of 32.9%. After this, pyrolytic decomposition of the organic moiety takes place, finishing around 700°C. The remaining weight is attributed to the formation of CdO (obsd, 17.36%; calcd, 17.1%).

In case of complex **3** in the 65–107°C temperature range weight loss effect is observed for dehydration involving the four coordinated water molecule (obsd, 9.45%; calcd, 10.01%). After that the complex shows the weight loss of 24.7% (calcd, 25.3%) with in temperature range 107–265°C at which two

pyridine molecules were expelled. This is followed by decomposition of the organic part till a constant weight, in which the CdO residue (obsd, 17.9%; calcd, 18.02%) is formed as final product.

Fluorescence properties

Photophysical properties of HDMV, **2** and **3** were studied using fluorescence spectroscopy. Fig. 15 shows the emission data of the compounds in aqueous solution at room temperature (10^{-4} M). The emission spectrum of HDMV at 314 nm displays three bands at 342, 407 and 428 nm. Emissions for benzimidazole are observed at 333, 423 and 457 nm ($\lambda_{\text{ex}} = 242$ nm) and pyridine is non-fluorescent.⁶⁴ The complexes exhibit emission peaks at 357, 419 and 440 nm upon excitation at 325 nm for **2** and 355, 423 and 450 nm upon excitation at 322 nm for **3**. Since the Cd²⁺ ions are difficult to oxidize or to reduce due to their d¹⁰ configuration these emission bands are neither metal-to-ligand charge transfer (MLCT) nor ligand-to-metal charge transfer (LMCT) in nature,⁶⁵ but rather can be attributed to intraligand emission. The fluorescence quantum yield (Φ) of HDMV, **2** and **3** are found to be 0.17, 0.39 and 0.23 respectively. Generally the band position, multiplicity and the emission quantum yield are strongly dependent on the structure and its rigidity of the underlying complex.⁶⁶

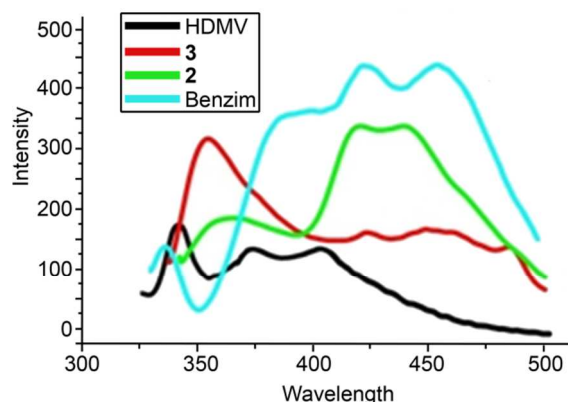


Fig. 14 Emission spectra of HDMV, Benzimidazole, **2** and **3**

Conclusions

In this present work, we synthesized and characterized *N,N'*-dimethylvioluric acid mono hydrate (HDMV) (**1**·H₂O) and two cadmium(II) complexes (**2** and **3**) obtained from reactions involving HDMV and different N-donor ligands (benzimidazole and pyridine). Hydrogen bond interactions are found to govern the primary structures. A common feature in compounds **1**·H₂O and **2** is the formation of a strong binding motif in the solid state dominated by an lp- π interaction. Moreover, in compound **2** this interaction together with a π -stacking interaction involving the benzimidazole coligand is responsible for the formation of a hexameric self-assembled supramolecular structure. From the DFT study in compound **1**·H₂O we have demonstrated that the molecular electrostatic

potential over the center of the ring is enhanced either by the intramolecular hydrogen bond or the presence of a water molecule in the same position than it has in the X-ray structure. The contributions of the different binding forces have been evaluated using several models that confirm the importance of both lp- π and π - π interactions. Finally, by means of the CSD search we have demonstrated the ability of the violuric ring to participate in π -interactions with neutral and anionic electron rich molecules.

Acknowledgements

We thank Dr. Frank Schaper [Département de chimie, Université de Montréal, Canada] for helpful comments regarding the X-ray structures. Financial assistance from Department of Biotechnology, Govt. of India [vide sanction No BCIL/NER-BPMC/2012.1549] is gratefully acknowledged. One of the authors R.B. is grateful to the authority of NIT-Agartala for providing Institute fellowship. A.B. and A.F. thank DGICYT of Spain (CTQ2011-27512/BQU and CONSOLIDER INGENIO CSD2010-00065, FEDER funds) and the Direcció General de Recerca I Innovació del Govern Balear (project 23/2011, FEDER funds) for funding. We thank the CTI (UIB) for free allocation of computer time. We also wish to acknowledge the anonymous reviewers whose comments and suggestions were exceedingly helpful during the revision process.

Notes and references

- ^aDepartment of Chemistry, National Institute of Technology (NIT)-Agartala, Tripura, India. Tel: +919612176571; E-mail: subrataorgchem@gmail.com
^bDepartament de Química, Universitat de les Illes Balears, Crta. de Valldemossa km 7.5, 07122 Palma de Mallorca (Balears), SPAIN; E-mail: toni.frontera@uib.es
^cPresent address: Department of Chemistry, National Institute of Technology (NIT) Patna, Ashok Rajpath, Patna-800005, Bihar, India Tel: +917677417481.

‡Both the authors have equal contribution to this work.

Electronic Supplementary Information (ESI) available: [Figures, IR, ¹H & ¹³C NMR and TGA data. CCDC reference numbers 1017331-1017333]. See DOI: 10.1039/b000000x/

1. C. D. Klaassen and J. Liu, *Drug Metab. Rev.*, 1997, **29**, 79–102.
2. M. Shibutani, K. Mitsumori, N. Niho, S. Satoh, H. Hiratsuka, M. Satoh, M. Sumiyoshi, M. Nishijima, Y. Katsuki, J. Suzuki, J. Nakagawa and M. Ando, *Arch. Toxicol.*, 2000, **74**, 571–577.
3. L. Chen, L. Lei, T. Jin, M. Nordberg and G. F. Nordberg, *Diabetes Care*, 2006, **29**, 2682–2687.
4. L. Friberg, C. G. Elinder, T. Kjellstrom, and G. F. Nordberg, *Cadmium and Health: A Toxicological and Epidemiological Appraisal*, eds CRC Press, Boca Raton, Florida, USA, 1985, vol. 2.
5. P. -A. Binz and J. H. R. Kägi, in *MetallothioneinIV*, ed. C. Klaassen, BirkhäuserVerlag, Basel, 1999, pp. 7–13.

6. T. W. Lane and F. M. M. Morel, *Proc. Natl. Acad. Sci.*, 2000 USA, **97**, 4627–4631.
7. P. X. Xi, Z. H. Xu, X. H. Liu and Z. Z. Zeng, *Spectrochim. Acta A*, 2008, **71**, 523–528.
8. E. Viñuelas-Zahinos, F. Luna-Giles, P. Torres-García and M. C. Fernández-Calderón, *Eur. J. Med. Chem.*, 2011, **46**, 150–159.
9. S. Bjelogrić, T. Todorovic, A. Bacchi, M. Zec, D. Sladić, T. Srdić-Rajić, D. Radanovic, S. Radulovic, G. Pelizzi and K. Andelkovic, *J. Inorg. Biochem.*, 2010, **104**, 673–682.
10. N. R. Filipovic, A. Bacchi, M. Lazic, G. Pelizzi, S. Radulovic, D. Sladić, T. R. Todorovic, and K. K. Andelkovic, *Inorg. Chem. Commun.*, 2008, **11**, 47–50.
11. H. Strasdeit, W. Saak, S. Pohl, W. L. Driessen, and J. Reedijk, *Inorg. Chem.*, 1988, **27**, 1557–1563.
12. S. K. Sahni and J. Reedijk, *Coord. Chem. Rev.*, 1984, **59**, 1–139.
13. D. L. Reger, J. E. Collins, S. M. Myers, A. L. Rheingold and L. M. Liable-Sands, *Inorg. Chem.*, 1996, **35**, 4904–4909.
14. H. Strasdeit, W. Saak, S. Pohl, W. L. Driessen and J. Reedijk, *Inorg. Chem.*, 1988, **27**, 1557–1563.
15. A. Domenicano, L. Torelli, A. Vaciago and L. Zambonelli, *J. Chem. Soc. A*, 1968, 1351–1361.
16. B.F. Hoskins and B.P. Kelly, *Inorg. Nucl. Chem. Lett.*, 1972, **8**, 875–878.
17. E. F. Epstein and I. Bernel, *J. Chem. Soc. A*, 1971, 3628–3631.
18. Z. Wang, R.-G. Xiong, B.M. Foxman, S. R. Wilson and W. Lin, *Inorg. Chem.*, 1999, **38**, 1523–1528.
19. F. A. Almeida Paz, Y. Z. Khimiyak, A. D. Bond, J. Rocha and J. Klinowski, *Eur. J. Inorg. Chem.*, 2002, **11**, 2823–2828.
20. F. Abraham, A. Nowogrocki, G. S. Sueur, and C. Bremard, *Acta Crystallogr.*, 1980, **B38**, 799–803.
21. M. Hamelin, *Acta Crystallogr.*, 1972, **B28**, 228–235.
22. K. Tamaki and N. Okabe, *Acta Crystallogr.*, 1996, **C52**, 1125–1127.
23. J. Faus, F. Lloret, M. Julve, J. M. Clemente-Juan, M. C. Munoz, X. Solans and M. Font-Bardía, *Angew. Chem.*, 1996, **35**, 1485–1487.
24. H. Gillier, *Bull. Soc. Chim.*, 1965, 2373–2384.
25. M. Hamelin, *Acta Crystallogr.*, 1976, **B32**, 364–370.
26. A. N. Illán-Cabeza, R. Antonio, G. Garcia, N. Miguel and M. Carretero, *Inorg. Chim. Acta*, 2011, **366**, 262–267.
27. J. Moratal and J. Faus, *Inorg. Chim. Acta*, 1977, **25**, L1–L3.
28. R.W. Awadallah, M. K. Sheriff and A. A. M. Gad, *J. Ind. Chem. Soc.*, 1984, **59**, 624–625.
29. M. Husain and Q. Husain, *Crit. Rev. Environ. Sci. Technol.*, 2008, **38**, 1–42.
30. N. A. Illán-Cabeza, A. R. García-García, J. M. Martínez-Martos, M. J. Ramírez-Expósito and M. N. Moreno-Carretero, *J. Inorg. Biochem.*, 2013, **126**, 118–127.
31. M. Kavlakova, A. Bakalova, G. Momekov and D. Ivanov, *Arzneimittelforschung*, 2012, **62**, 599–602.
32. M. A. R. Molina, J. D. M. Ramos, J. d. D. L. Gonzalez and C. V. Calahorra, *An. Quim.*, 1983, **79**, 200–206.
33. C. Ruiz-Valero, A. Monge, E. Gutierrez-Puebla and E. Gutierrez-Rios, *Acta Crystallogr.*, 1984, **C40**, 811–812.
34. M. A. Romero, J. M. Salas, M. Simard, M. Quirós and A. L. Beauchamp, *Polyhedron*, 1990, **9**, 2733–2739.
35. N. A. Illán-Cabeza, A. R. García-García and M. N. Moreno-Carretero, *Inorg. Chim. Acta*, 2011, **366**, 262–267.
36. E. Colacio, C. López-Magaña, V. McKee and A. Romerosa, *J. Chem. Soc., Dalton Trans.*, 1999, 2923–2926.
37. R. Rusakowicz and A. C. Testa, *J. Phys. Chem.*, 1968, **72**, 2680–2681.
38. SAINT, Data Reduction and Frame Integration Program for the CCD Area-Detector System. Bruker Analytical X-ray Systems, Madison, Wisconsin, USA, 1997–2006.
39. G. M. Sheldrick, *SADABS, Program for area detector adsorption correction*, Institute for Inorganic Chemistry, University of Göttingen, Germany, 1996.
40. O. V. Dolomanov, L. J. Bourhis, R. J. Gildea, J. A. K. Howard and H. Puschmann, *J. Appl. Crystallogr.*, 2009, **42**, 339–341.
41. G. M. Sheldrick, *Acta Crystallogr.*, 2008, **A64**, 112–122.
42. A. L. Spek, *J. Appl. Crystallogr.*, 2003, **36**, 7.
43. R. Ahlrichs, M. Bär, M. Hacer, H. Horn and C. Kömel, *Chem. Phys. Lett.*, 1989, **162**, 165–169.
44. S. Grimme, J. Antony, S. Ehrlich, and H. Krieg, *J. Chem. Phys.*, 2010, **132**, 154104–19.
45. A. Aydın, O. Ercan, S. Tascioglu, *Talanta*, 2005, **66**, 1181–1186.
46. F. Bélanger-Gariépy, R. Faure, F. Hueso-Ureña, M. N. Moreno-Carretero, J. A. Rodríguez-Navarro and J. M. Salas-Peregrín, *Polyhedron*, 1998, **17**, 1747–1753.
47. G. S. Nichol and W. Clegg, *Acta Crystallogr.*, 2005, **C61**, o721–o724
48. G. S. Nichol and W. Clegg, *Acta Crystallogr.*, 2005, **C61**, o718–o721.
49. G. S. Nichol, and W. Clegg, *Acta Crystallogr.*, 2005, **E61**, o3788–o3725.
50. K. Guille, R. W. Harrington and W. Clegg, *Acta Crystallogr.*, 2007, **C63**, o327–o329.
51. V. Bertolasi, P. Gilli, V. Ferretti and G. Gilli, *New J. Chem.*, 2001, **25**, 408–415.
52. K. Tamaki and N. Okabe, *Acta Crystallogr.*, 1996, **C52**, 1125–1127.
53. M. Hamelin, *Acta Crystallogr.*, 1972, **B28**, 228–235.
54. K. Tamaki and N. Okabe, *Acta Crystallogr.*, 1996, **C52**, 1124–1125.
55. F. H. Allen, *Acta Crystallogr.*, 2002, **B58**, 380–388.
56. M. Cameron, B. G. Gowenlock and G. Vasapollo, *J. Organomet. Chem.*, 1991, **403**, 325–333.
57. A. Nangia, K. Biradha and G. R. Desiraju, *J. Chem. Soc., Perkin Trans.*, 1996, **2**, 943–953.
58. A. Frontera, P. Gamez, M. Mascal, T. J. Mooibroek and J. Reedijk, *Angew. Chem., Int. Ed.*, 2011, **50**, 9564–9583;
59. R. Kivekas, A. Pajunen, E. Colacio, J. M. Dominguez-Vera, J. M. Moreno and A. Romerosa, *Acta Chem. Scand.* 1997, **51**, 1051–1057.
60. J. Faus, M. Julve, F. Lloret, J. A. Real and J. Sletten, *Inorg. Chem.* 1994, **33**, 5535–5540.
61. A. Frontera, *Coord. Chem. Rev.* 2013, **257**, 1716–1727.
62. J. J. Fiol, M. Barcelo-Oliver, A. Tasada, A. Frontera, A. Terron and A. Garcia-Raso, *Coord. Chem. Rev.*, 2013, **257**, 2705–2715.
63. K. Wang, H. -H. Zou, Z. -L. Chen, Z. Zhang, W. -Y. Sun and F. -P. Liang, *Dalton Trans.*, 2014, 43, 12989–12995.
64. I. Yamazaki and H. Baba, *J. Chem. Phys.*, 1977, **66**, 5826–5827.
65. W. Yuan, T. Liu, Z. Guo, H. Li and R. Cao, *J. Mol. Struct.*, 2010, **965**, 82–88.
66. A. Bhattacharya, S. Majumder, J. P. Naskar, P. Mitra and S. Chowdhury, *J. Coord. Chem.*, 2014, **67**, 1413–1428.

The synthesis and X-ray characterization of two *N,N'*-dimethylvioluric acid (**1**) derivatives of formula $[\text{Cd}(\text{DMV})_2(\text{Benzim})_2]$ (**2**) (Benzim= benzimidazole) and $[\text{Cd}(\text{H}_2\text{O})_4(\text{py})_2](\text{DMV})_2$ (**3**) (py= pyridine). They present interesting assemblies in the solid state dominated by H-bonding, π - π and $\text{lp}-\pi$ interactions.

